Excitation of spin waves by a current-driven magnetic nanocontact in a perpendicularly magnetized waveguide

Giancarlo Consolo, Luis Lopez-Diaz, Bruno Azzerboni, Ilya Krivorotov, Vasil Tiberkevich, and Andrei Slavin

Phys. Rev. B **88**, 014417 — Published 17 July 2013

DOI: 10.1103/PhysRevB.88.014417

Excitation of spin waves by a current-driven magnetic nanocontact in a perpendicularly magnetized waveguide

Giancarlo Consolo[1], Luis Lopez-Diaz[2], Bruno Azzerboni[3], Ilya Krivorotov[4], Vasil Tiberkevich[5] and Andrei Slavin[5]

[1] Department of Mathematics and Computer Science, University of Messina, 98166 Messina, Italy

[2] Department of Applied Physics, University of Salamanca, 37008 Salamanca, Spain

[3] Department of Electronic Engineering, Industrial Chemistry and Engineering, , University of Messina, 98166 Messina, Italy

[4] Department of Physics and Astronomy, University of California, 92697 Irvine, USA

[5] Department of Physics, Oakland University, Rochester, Michigan 48309, USA

Abstract

It is demonstrated both analytically and numerically that the properties of spin wave modes excited by a current-driven nano-contact of length L in a quasi-one-dimensional magnetic waveguide magnetized by a perpendicular bias magnetic field H_e are qualitatively different from the properties of spin waves excited by a similar nano-contact in a two-dimensional unrestricted magnetic film ("free layer"). In particular, there is an optimum nano-contact length L_{opt} corresponding to the minimum critical current of the spin wave excitation. This optimum length is determined by the magnitude of H_e, the exchange length and the Gilbert dissipation constant of the waveguide material. Also, for $L < L_{opt}$ the wavelength λ (and the wave number k) of the excited spin wave can be controlled by the variation of H_e (λ decreases with the increase of H_e), while for $L > L_{opt}$ the wave number k is fully determined by the contact length L (k~1/L) , similar to the case of an unrestricted two-dimensional "free layer".

I. Introduction

The geometry of magnetic nanostuctures used to construct spin-torque nano-oscillators (STNO) (see e.g. [1]) could have a strong influence on the properties of spin wave modes excited in these STNO structures by the spin-transfer torque [2,3] carried by the spin-polarized current. Traditionally, two main geometries - magnetic nano-contacts [4,5] and magnetic nano-pillars [6] - where used. In the nano-contact geometry, the STNO "free layer" (where the current-induced precession of magnetization takes place) is a continuous magnetic film unrestricted in both in-plane dimensions. In this geometry, depending on the direction of the bias magnetic field, spin-polarized current excites usually either propagating spin waves, having the wavenumber determined by the nanocontact radius [7-10], or a self-localized nonlinear bullet mode [10-12], having the frequency that is below the spectrum of propagating spin waves. It should be noted that it is also possible to excite other types of spin wave modes (e.g., magnetic droplet solitons [13,14]) or to excite spin waves in magnetic nano-structures by other means (e.g., by specially prepared light pulses [15,16]) and achieve a certain level of control of the wavelength of the excited spin waves. However, these methods of spin wave excitation mostly deal with the highly-nonlinear solitonic spin wave modes for which independent control of the wavelength and amplitude is impossible.

In the case of a nano-pillar geometry the "free" magnetic layer has finite lateral sizes and reflecting boundaries in the plane of the layer and represents a thin magnetic resonator [6]. The spin wave eigenmodes of this resonator, that have discrete frequencies determined by the finite in-plane sizes of the pillar, can be excited by the traversing spin-polarized current.

There is, however, another STNO geometry which might be useful for the development of novel microwave signal processing devices based on the spin-transfer torque effect [17-18] (see Fig.1). In this geometry the "free" layer of STNO has a shape of a quasi-one-dimensional waveguide, where spin waves excited by a nano-contact attached to the waveguide can propagate and provide a synchronization signal for other nano-contacts attached to the same waveguide, thus forming a

synchronized linear STNO array with enhanced output power and reduced generation linewidth [19].

The main goal of our current paper was to study analytically and numerically the properties of spin wave modes excited by a current-driven magnetic nano-contact in such a quasi-one dimensional magnetic waveguide and to analyze the potential of this geometry for the development of practical spintronic microwave devices. Our analysis demonstrates that the properties of spin wave modes excited by a current-driven nano-contact of the length L in a quasi-one-dimensional magnetic waveguide magnetized by a perpendicular bias magnetic field H_e (see Fig.1) are qualitatively different from the properties of spin waves excited by a similar nano-contact in two-dimensional unrestricted magnetic film [7]. In particular, there is an optimum nano-contact length L_{opt} corresponding to the minimum critical current of the spin wave excitation. This optimum length is determined by the magnitude of H_e, the exchange length and the Gilbert dissipation constant of the waveguide material. Also, for $L < L_{opt}$ the wave number k of the excited spin wave can be controlled by the variation of H_e (k decreases with the decrease of H_e), while for $L > L_{opt}$ the wave number k is fully determined by the contact length L ($k \sim 1/L$) , similar to the case of an unrestricted two-dimensional "free layer" [7].

II. Analytical Model

The core of the device geometry under investigation is a trilayer structure composed by an extended thick magnetic layer (the "pinned layer" (PL)), a non-magnetic spacer and a thin magnetic layer (the "free layer" (FL)) in the form of a thin quasi-one-dimensional waveguide (prism) elongated along one direction (the x-axis), but confined along the other two directions (see Fig.1). A metallic contact of finite length L attached to the top of the FL allows the current flow perpendicular to the layers in a confined region of the trilayer, as shown in Fig.1. We also assume that the waveguide is magnetized to saturation by the bias magnetic field of the magnitude H_e directed along the axis z.

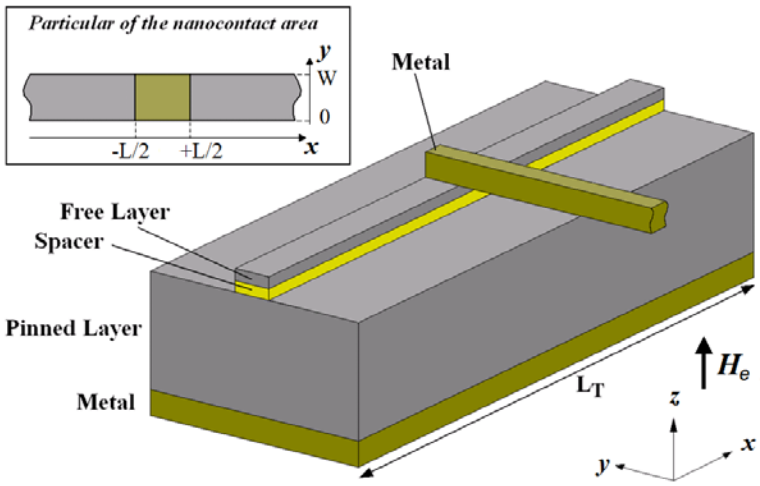

Fig.1. The geometry of the STNO with the "free layer" in the form of a perpendicularly magnetized magnetic waveguide of the finite width *W*.
In the top-left inset the geometry of the nano-contact of a finite length *L* is shown in detail.

In contrast with the classical nano-contact geometry [7,12,20-21], where the spin-wave mode excited by a nano-contact can propagate radially in the unrestricted two-dimensional "free" layer, in this case the excited spin waves can only propagate along the axis "x" of a quasi-one-dimensional waveguide. This reduction of dimensionality in the wave propagation has a profound effect on the properties of spin wave modes excited in this waveguide geometry.

The equation of motion for the magnetization vector $\mathbf{M}$ in the waveguide "free" layer (Landau-Lifshitz-Gilbert-Slonczewski equation) can be written in the form :

$$\frac{\partial \mathbf{M}}{\partial t} = \gamma\left[\mathbf{H}_{\text{eff}} \times \mathbf{M}\right] + \frac{\alpha_G}{M_0}\left[\mathbf{M} \times \frac{\partial \mathbf{M}}{\partial t}\right] + \Theta(L/2 - |x|)\frac{\beta I}{M_0 L}\left[\mathbf{M} \times (\mathbf{M} \times \mathbf{p})\right], \qquad (1)$$

where $\mathbf{M} = \mathbf{M}(t, \mathbf{r})$ is the magnetization vector of the FL (we are neglecting dynamics in the PL), γ is the modulus of the gyromagnetic ratio for the electron spin, $\mathbf{H}_{\text{eff}} = (H_e - 4\pi M_z)\,\mathbf{z} - \lambda_{ex}^2 \nabla^2 \mathbf{M}$ is the effective magnetic field which includes Zeeman, dipole-dipole and exchange contributions, M_0 and λ_{ex} are the magnitude of the static magnetization and the exchange length in the waveguide (FL) material, respectively, and M_z is the *z*- projection of the FL magnetization that coincides with M_0 in the static case. It is assumed that the thickness d_{FL} of the "free" layer waveguide is much smaller than its width *W,* so that the waveguide is considered to be quasi-one-dimensional. The

effects arising from the current-induced (Oersted) magnetic field, magnitocrystalline anisotropy, magnetostatic coupling between the two ferromagnetic layers and the thermal fluctuations are also neglected as they do not play a significant role in this context [20,22]. The first term on the right-hand side of Eq.(1) represents, therefore, the conservative precessional torque.

The second term in the right-hand side of (1) is the magnetic damping torque written in the traditional Gilbert form (α_G is the damping constant) of the FL material. The last term is the Slonczewski spin-transfer torque that is proportional to the bias current *I*. The function $\Theta(L/2-|x|)$ describes the spatial distribution of the current across the nano-contact area (of the length *L*). The coefficient β characterizing the strength of the spin-transfer torque is related to the dimensionless spin-polarization efficiency ε ($0<\varepsilon<1$) by the expression $\beta=\varepsilon g\mu_B/2eM_0Wd_{FL}$, where *g* is the spectroscopic Landé factor, μ_B is the Bohr magneton, *e* is the absolute value of the electron charge, d_{FL} is the FL thickness and W is the waveguide width (along the *y* axis). Note that in this formulation the coefficient β is independent of the nano-contact length *L*. The unit vector **p** defines the spin-polarization direction which coincides with the equilibrium direction of the PL magnetization. In our analysis, we assume that the directions of the static magnetization of the two layers are parallel to each other. In the first approximation, the misalignment of equilibrium magnetization orientations in the two layers leads simply to the reduction of the effective spin-polarization efficiency, *i.e.* to the scaling of the critical current. Since we are considering normally-to-plane bias fields, we thus assumed that $\mathbf{p}=\mathbf{z}$.

Introducing the dimensionless complex variable a

$$a=\frac{M_x-i\,M_y}{\sqrt{2M_0(M_0+M_z)}}\quad , \tag{2}$$

proportional to the amplitude of the magnetization precession in the FL (where M_i, with $i=x,y,z$, are the Cartesian projections of the FL magnetization vector **M**) one can rewrite Eq.(1) in the following form (for the details of the derivation see [23]):

$$\frac{\partial a}{\partial t} = -i\left(\omega_0 - D\frac{\partial^2}{\partial x^2}\right)a - \Gamma\, a + \Theta(L/2 - |x|)\frac{\beta\, I}{L}\, a \ , \tag{3}$$

where ω_0 is the ferromagnetic resonance (FMR) frequency in the perpendicularly magnetized (along the axis z in Fig.1) thin ($d_{FL} << W$) FL:

$$\omega_0 = \gamma\left(H_e - 4\pi M_0\right) \ , \tag{4}$$

$D = \gamma 4\pi M_0 \lambda_{ex}^2$ is the dispersion coefficient of the exchange-dominated spin waves excited in the nano-contact, $\lambda_{ex} = \sqrt{A/2\pi M_0^2}$, A is the exchange constant, and $\Gamma = \alpha_G\, \omega_0$ is the FMR linewidth proportional to the FL Gilbert damping constant α_G. Only the terms linear in the spin wave amplitude a were retained in Eq. (3): the nonlinear corrections, which can also be obtained using ansatz Eq. (2), do not influence the threshold of spin wave generation and do not change the profile or frequency of the excited mode at the threshold. Eq. (3) correctly describes spin wave dynamics only when $H_e > 4\pi M_0$, and the saturated state of the waveguide is stable; below, we restrict our analysis only to this case.

The stationary solution of Eq.(3) at the threshold of the current-induced spin wave generation can be found in the form:

$$a(t,x) = e^{-i\omega_g t}\begin{cases} \cos(\kappa\, x), & |x| < L/2 \\ \cos(\kappa\, L/2)\, e^{i\,k(|x|-L/2)}, & |x| > L/2 \end{cases} \tag{5}$$

where κ and k are the complex wave numbers of the spin wave modes excited inside and outside the current-carrying nano-contact region and ω_g is the frequency of the excited spin waves. The imaginary parts of the wave numbers κ and k describe the energy loss/gain of the excited spin wave mode. Using the condition of continuity for the variable spin wave amplitude $a(t,x)$ at the boundaries of the nano-contact region one can obtain the following system of equations defining the complex spin wave wave numbers κ and k, the frequency ω_g of the excited spin wave and the threshold current I_{th} at which the current-induced spin wave excitation starts in the nano-contact :

$$\omega_g = \omega_0 + D\,\kappa^2 - i\left(\Gamma - \frac{\beta\, I_{th}}{L}\right)\ , \tag{6a}$$

$$\omega_g = \omega_0 + D\,k^2 - i\,\Gamma\ \ , \tag{6b}$$

$$\kappa \tan(\kappa\, L/2) = -i\,k\ . \tag{6c}$$

The system of equations (6) can not be solved analytically in a general case, but if we introduce the characteristic length scale ℓ_c of the problem as:

$$\ell_c = \sqrt{\frac{4D}{\Gamma}} = \frac{2\lambda_{ex}}{\sqrt{\alpha_G}} \frac{1}{\sqrt{(H_e / 4\pi M_0) - 1}}\ , \tag{7}$$

and the characteristic current I_c as:

$$I_c = \frac{\Gamma}{\beta}\ell_c\ \ , \tag{8}$$

it is possible to find approximate analytical solutions of the problem in two limiting cases.

In the limiting case of a "long" nano-contact $L >> \ell_c$, when the spin wave propagation is dominated by the Gilbert losses, the approximate solution of (6) has the form:

$$I_{th} = I_c \frac{L}{\ell_c}\ , \qquad k = \frac{\pi}{L}, \qquad \omega_g = \omega_0 + D\left(\frac{\pi}{L}\right)^2. \tag{9}$$

In the opposite limiting case of a "short" $L << \ell_c$ nano-contact, when the spin wave propagation is dominated by the propagation losses, the approximate solution of (6) has the form:

$$I_{th} = I_c\left(\frac{3\,\ell_c}{4\,L}\right)^{1/3}, \quad k = \left(\frac{6}{L\,\ell_c^{\,2}}\right)^{1/3} = \frac{1}{(L\lambda_{ex}^2)^{1/3}}\left[\frac{3\alpha_G}{2}\left(\frac{H_e}{4\pi M_0} - 1\right)\right]^{1/3}, \ \omega_g = \omega_0 + D\left(\frac{6}{L\,\ell_c^2}\right)^{2/3}. \tag{10}$$

It is clear from the expressions for critical current in (9) and (10) that there should be an optimum value of the nano-contact length $L_{opt} \sim \ell_c$, at which the critical current has the minimum value $I_{th}^{\min} \sim I_c$. The exact values of L_{opt} and $I_{th}^{\min}$ can be found from numerical solution of equations (6):

$$L_{opt} \approx 0.52\ell_c\,, \tag{11}$$

$$I_{th}^{\min} \approx 1.48 I_c\ . \tag{12}$$

The typical values of ℓ_c lie in the range of 50-100 nm for applied fields H_e about 2 times higher than the saturation field $4\pi M_0$.

It is also clear from the expressions (9) and (10) for the wavenumber k of the spin wave mode propagating from the nano-contact that for a "long" contact (9) the wavenumber is totally determined by the nano-contact size L, while for a "short" contact (10) it is possible to control the value of k by variation of the external bias magnetic field H_e. This latter regime is qualitatively different from the case of nano-contact radiation of spin waves in a two-dimensional "free" layer and could be used to enhance the group velocity of spin waves propagating in a waveguide , thus improving the possibility of mutual synchronization of several generating nano-contacts connected to the same waveguide "free" layer [19].

III. Micromagnetic Model

To check the above presented approximate analytical results we performed the numerical study of the spin-torque-induced excitation and propagation of spin waves in a magnetic waveguide by means of finite-difference micromagnetic scheme [12,20-21,24-25] which integrates, in the time domain, the Landau-Lifshitz-Gilbert-Slonczewski equation of motion (1). In our numerical study we used the following parameters of the nano-contact device Fig.1 : exchange constant A_{ex} = 1.4×10^{-6} erg/cm , saturation magnetization $4\pi M_0$ = 8 kG, lateral sizes of the PL $L_T \times L_T$ = 3μm × 3μm and thickness d_{PL} = 70 nm, lateral sizes of the FL $L_T \times W$ =3μm × 69 nm and thickness d_{FL} = 3 nm (the corresponding integration cell is a cube with a side of 3 nm), Gilbert damping constant α_G=0.02, spin-torque efficiency ε = 0.3. It was assumed that the current-carrying region has a fixed width W = 69 nm along the y axis, while the x dimension (nano-contact length L) is varied. The current density was assumed to be uniform within the $W\times L$ area and zero outside. The strength of the external bias magnetic field H_e was varied in the range (8 – 20) kOe.

IV. Comparison between micromagnetic and analytic results and discussion

In the course of our micromagnetic study, first, we calculated the dependences of the bias current I_{th} and the spin wave frequency $f_g = \omega_g / 2\pi$, both computed at the threshold of spin wave generation, as functions of the external bias magnetic field H_e for the nano-contact of the length L= 69 nm. The results of these micromagnetic calculations are presented in Fig.2a,b as dots. In the same figures we present the results of numerical solution of the analytical model equations (6) as solid lines.

As one can see from Fig. 2, the dependences of the analytically calculated threshold current and generated frequency on the bias field have the same form as the micromagnetically calculated ones, but are shifted to the right by approximately 0.2 T. This shift is explained by the finite sizes of the magnetic waveguide in the simulations, which leads to finite demagnetization factors of the waveguide. As a result, the ferromagnetic resonance frequency (and, respectively, Gilbert damping which determines threshold current) is not described by the simple Eq. (4), but has more complicated form (see Eq. (14) below), which can be approximated by the shift of the bias field.

In addition, we note that the linear slope $\partial f_g / \partial H_e \simeq 27.4$ GHz/T of the micromagnetically calculated curve $f_g = f(H_e)$ presented in Fig.2b agrees quite well with the value of the gyromagnetic ratio γ for electron spin which follows from (13),(14).

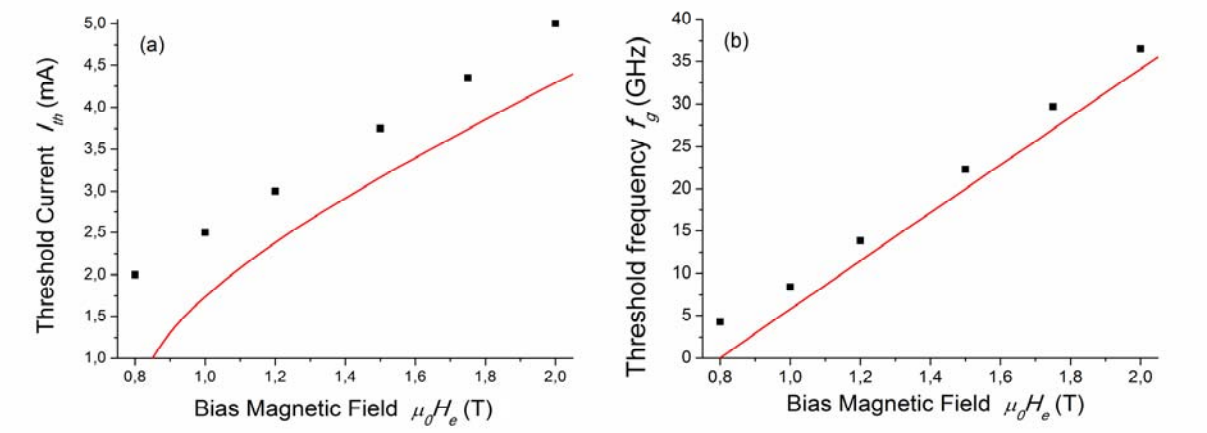

Fig.2. Dependence of the current I_{th} (a) and generation frequency $f_g = \omega_g / 2\pi$ (b), computed at the threshold, on the magnitude of the bias magnetic field H_e. Dots: numerical simulation, solid lines: analytic theory from Eqs.(6).

Then, we calculated the dependence of the generation frequency $f_g = \omega_g / 2\pi$ on the applied bias current at the fixed magnitude of the bias magnetic field H_e = 10 kOe and fixed nano-contact length L = 69 nm from the micromagnetic simulations in (1) and from the numerical solution of the model equation (3). The results of these calculations are presented in Fig.3. It is clear that the generation frequency increases with current, like it should in the case of a perpendicular magnetization of the free layer, and demonstrates nonlinear behavior at larger current magnitudes. Micromagnetic results (dots) show that the excitation of spin waves by direct current exhibits no hysteresis. It is also clear from Fig.3 that micromagnetic results (dots) reproduce well the results of the numerical solution of the model equation (3) (solid line).

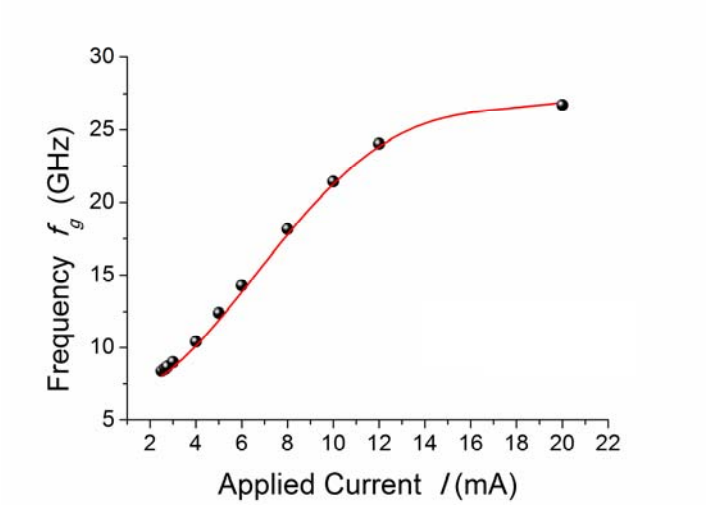

Fig.3. Dependence of the generated frequency $f_g = \omega_g / 2\pi$ on the applied current I at the fixed value of the bias magnetic field of H_e = 10 kOe and fixed length L = 69 nm of the nano-contact.

Dots: micromagnetic simulation, solid line: numerical solution of the model equation (3).

It is important to note that the micromagnetically calculated generation frequency f_g can be well described by the classical expression for the frequency of exchange-dominated spin waves:

$$\omega_g = \omega_{0p} + Dk_{num}^2 \tag{13}$$

where ω_{0p} is the FMR frequency of the perpendicularly magnetized FL waveguide (taken as a rectangular prism) and $k_{num}=2\pi/\lambda_{num}$ is the numerically calculated wavenumber (where λ_{num} is the wavelength of the generated spin wave). The FMR frequency in the waveguide $\omega_{0p} \simeq \omega_0$ is computed from the expression [see Eq.(2) in Ref. 26]:

$$\omega_{0p} = \gamma\sqrt{\left(H_e + (N_{xx} - N_{zz})4\pi M_0\right)\left(H_e + (N_{yy} - N_{zz})4\pi M_0\right)} \quad , \tag{14}$$

where N_{ii} ($i = x,y,z$) are the demagnetizing factors of a rectangular prism. The numerical values of the prism demagnetization factors N_{xx}=0.0014 and N_{yy}=0.0638 are much smaller than that of N_{zz}=0.9348, so Eq.(14) gives a result $f_{0p} = \omega_{0p}/2\pi = 7.76$ GHz that is very close numerically to the result obtained from the simple approximate expression (4).

Also, if for each value of the bias direct current I we determine from the micromagnetic simulations the wavenumber k_{num} of a spin wave excited in the waveguide nano-contact and, then, use these values in Eq.(13), we get the frequencies of generated spin waves that agree very well (the difference is less than 300 MHz) with the frequencies obtained from both the micromagnetic simulations and the numerical solution of the model equation (3).

Our micromagnetic simulations also allow us to determine the spatial profile of the excited spin wave mode and to confirm the propagating character of this mode. For example, the micromagnetically simulated profile of the spin-wave power P (proportional to the square of the envelope amplitude A ($P \sim A^2$) of the y-component of the normalized magnetization) as a function of the distance r from the nano-contact center is shown in Fig.4 by dots.

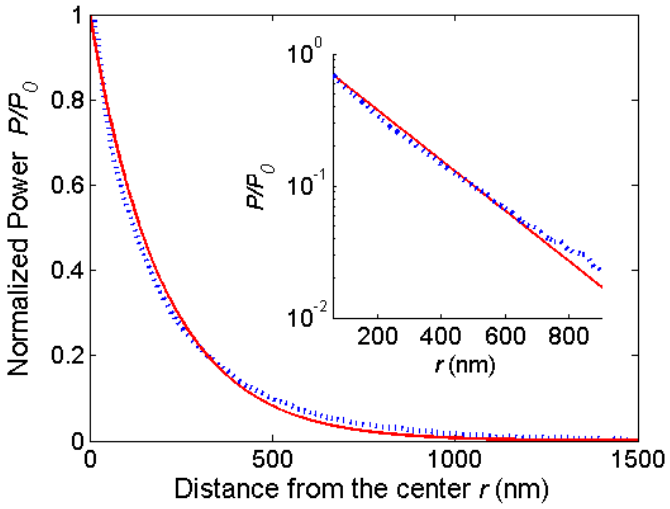

Fig.4. Dependence of the normalized spin-wave power (P/P_0) on the distance r from the center of a nano-contact at the applied current I = 4 mA and bias magnetic field $\mu_0 H_e$ = 1 T. The dotted line is the result of micromagnetic simulations, while the solid line corresponds to an exponential fit $P(r)/P_0 = \exp(-2r/\rho)$ with $\rho = 455$ nm . The inset shows the same graph as in the main panel with the normalized power expressed in a logarithmic scale.

It is clear from Fig.4 (and in particular by the log-scale inset), the normalized power of the excited spin wave mode exhibits an exponential decay which is well described by the expression $P(r)/P_0 = (A/A_0)^2 = \exp(-2r/\rho)$ where the characteristic spin wave "propagation distance" ρ

(distance at which the spin wave amplitude A reduces e-times) characterizing the spin wave propagation losses in the Py waveguide is determined from the comparison with the micromagnetic results to be $\rho = 455$ nm (see Fig.4). The propagation distance ρ can be also approximately calculated quasi-analytically, assuming that it is equal to the ratio between the spin wave group velocity v_g and the effective damping rate Γ and determining the spin wave wave number k_{num} from micromagnetic simulations:

$$\rho = \frac{v_g}{\Gamma} = \frac{\partial \omega_g / \partial k}{\alpha_G \omega_g} = \frac{2Dk_{num}}{\alpha_G(\omega_{0p} + Dk_{num}^2)} \tag{15}$$

Using the analytical expression $D = \gamma 4\pi M_0 \lambda_{ex}^2$ =7740 GHz·nm^2 for the exchange stiffness, Eq.(14) for the FMR frequency $\omega_{0p}/2\pi$=10.5 GHz, nominal value α_G = 0.02 for the Gilbert damping constant, and micromagnetically calculated at I =4 mA (as in Fig.4) value of the spin wave wavenumber k_{num} = 0.042 nm^{-1} (λ_{num}=150 nm) one obtains the value $\rho \simeq 490\ nm$, which turns out to be in a reasonably good agreement with the above presented micromagnetic result.

The most interesting and non-trivial result obtained in our micromagnetic simulations performed for the quasi-one-dimensional waveguide geometry is the confirmation of the non-monotonic dependence of the threshold current I_{th} on the nano-contact length L, for a fixed value of the bias magnetic field (H_e = 10 kOe). It follows from the above developed analytic theory (6)-(12) that the dependence of the bias current I_{th} on the nano-contact length L should have a minimum value $I_{th}^{\min} \sim I_c$ near the point where $L \simeq \ell_c$ (see (11), (12)), and qualitatively different behaviour of I_{th} below and above this point (see (9) and (10)). All these conclusions of the analytic theory were fully confirmed in out micromagnetic simulations, the results of which are presented in Fig.5. Indeed, Fig.5 demonstrates a pronounced minimum in the threshold current at the nano-contact length L = 102 nm which is very close to the analytically predicted value $L_{opt} \simeq \ell_c$ = 105 nm following from (7).

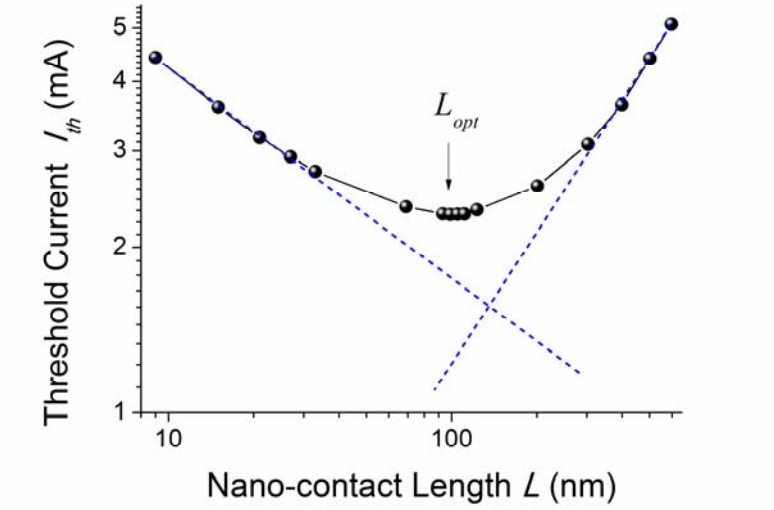

Fig.5. Dependence (double logarithmic scale) of the threshold current I_{th} on the nano-contact length L micromagnetically calculated (dots) for the fixed value of the bias magnetic field H_e = 10 kOe. The solid line is the guide for the eye. The dashed lines are the asymptotic theoretical dependences calculated using Eq. (10) for $L < \ell_c$ and Eq.(9) for $L > \ell_c$ ($\ell_c = 105\,\text{nm}$).

Also the micromagnetically calculated behaviour of the threshold current in the regions $L << L_{opt}$ and $L >> L_{opt}$ agrees remarkably well with the analytic predictions, Eqs. (10) and (9), respectively (see dashed lines in Fig.5).

There is another non-trivial feature of the considered quasi-one-dimensional geometry of the free layer Fig.1. In contrast with the case of a finite-radius nano-contact in a two-dimensional free layer, where the wavelength of the spin wave excited at the threshold is determined exclusively by the nano-contact radius R_c ($\lambda_{th} \sim 4.5R_c$) [7], in the case of a short ($L < L_{opt}$) nano-contact in a waveguide the wavelength λ (or the wave number k) of the excited spin wave can be also controlled by varying the strength of the bias magnetic field H_e (see Eqs. (10). This interesting feature analytically predicted in (10) provides an additional degree of freedom to manipulate the properties of the excited spin waves. This theoretical prediction is also confirmed in our micromagnetic simulations (see Fig.6) performed for a "short" ($L < L_{opt}$) nano-contact of the length

L = 69 nm . It is clear from Fig.6 that the micromagnetically calculated wavelength of the spin wave excited at the threshold (dots in Fig.6) can be reduced two times when the bias magnetic field H_e is increased from 10 kOe to 20 kOe. The analytic result from (10) (shown as a solid line in Fig.6) is in a reasonably good agreement with the simulation results.

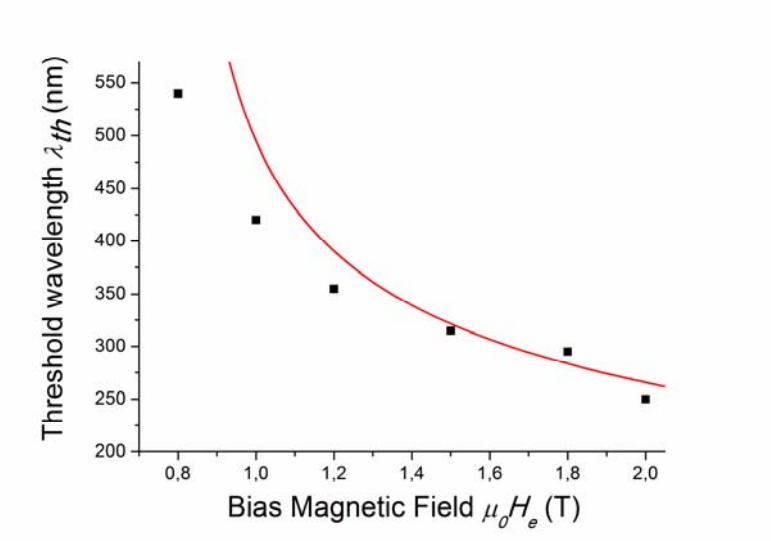

Fig.6. Dependence of the spin wave wavelength λ_{th} at the excitation threshold on the magnitude of the bias magnetic field H_e calculated for the "short" ($L < L_{opt}$) nano-contact nano-contact of the length L = 69 nm micromagnetically (dots) and analytically from (10) (solid line).

V. Conclusions

In conclusion, our analytic and micromagnetic study of the spin-transfer driven excitation of spin wave modes in a quasi-one-dimensional magnetic waveguide demonstrated two new features of this geometry in comparison with the traditional two-dimensional nano-contact geometry [7]: (i) the dependence of the threshold bias current on the nano-contact length is non-monotonous and has a minimum defined by Eqs. (11), (12); (ii) for "short" ($L < L_{opt}$) nano-contacts it is possible to control the wavelength of the radiated spin wave by varying the magnitude of the bias magnetic field. This last feature might be very important for the experimental study of the spin wave propagation in magnetic waveguides as by the variation of the bias field the spin wave wavelength could be brought to the region λ >300 nm where the wave process is accessible for the observation

by the micro-focus Brillouin light scattering [8,9]. The same feature might also be useful for the development of the synchronized linear arrays of nano-contact STNOs, as by variation of the wavelength one can also vary the spin wave group velocity (and , therefore, the spin wave propagation distance ρ (15). That way by varying the bias magnetic field H_e it would be possible to vary the effective coupling between the nano-contact STNO and, thus, influence the synchronization properties of the linear STNO array.

Acknowledgments

The paper was supported by MIUR-PRIN 2010-11 under Project 2010ECA8P3 "DyNanoMag" and by a Spanish Project under Contract No. MAT2011-28532-C03-01.

References

[1] A. Slavin and V. Tiberkevich, IEEE Trans. Magn. **45**, 1875 (2009)

[2] J. C. Slonczewski, J. Magn. Magn. Mater. **159**, L1 (1996)

[3] L. Berger, Phys. Rev. B **54**, 9353 (1996)

[4] M. Tsoi, A. G. M. Jansen, J. Bass, W. C. Chiang, M. Seck, V. Tsoi, and P.Wyder, Phys. Rev. Lett. **80**, 4281 (1998)

[5] W. H. Rippard, M. R. Pufall, S. Kaka, S. E. Russek, and T. J. Silva, Phys. Rev. Lett. **92**, 027201 (2004)

[6] S. I. Kiselev, J. C. Sankey, I. N. Krivorotov, N. C. Emley, R. J. Schoelkopf, R. A. Buhrman, and D. C. Ralph, Nature **425**, 380 (2003)

[7] J. C. Slonczewski, J. Magn. Magn. Mater. **195**, L261 (1999)

[8] V.E. Demidov, S. Urazhdin, S.O. Demokritov, Nature Mater. **9**, 984(2010)

[9] M. Madami, S. Bonetti, G. Consolo, S. Tacchi, G. Carlotti, G. Gubbiotti, F. B. Mancoff, M. A. Yar and J. Åkerman, Nature Nanotechnology **6**, 635 (2011)

[10] S. Bonetti, V. Tiberkevich, G. Consolo, G. Finocchio, P. Muduli, F. Mancoff, A. Slavin, J. Akerman, Phys. Rev. Lett. **105**, 217204 (2010)

[11] A. Slavin and V. Tiberkevich, Phys. Rev. Lett. **95**, 237201 (2005)

[12] G. Consolo, B. Azzerboni, L. Lopez-Diaz, G. Gerhart, E. Bankowski, V. Tiberkevich and A. N. Slavin, Phys. Rev. B **78**, 014420 (2008)

[13] M.A. Hoefer, T.J. Silva, M.W. Keller, Phys. Rev. B **82**, 054432 (2010)

[14] S.M. Mohseni, S. R. Sani, J. Persson, T. N. Anh Nguyen, S. Chung, Ye. Pogoryelov, P. K. Muduli, E. Iacocca, A. Eklund, R. K. Dumas, S. Bonetti, A. Deac, M. A. Hoefer, J. Åkerman, Science **339**, 1295 (2013)

[15] T. Satoh, Y. Terui, R. Moriya, B.A. Ivanov, K. Ando, E. Saitoh, T. Shimura, K. Kuroda, Nature Photonics **6**, 662 (2012)

[16] Y. Au, M. Dvornik, T. Davison, E. Ahmad, P. S. Keatley, A. Vansteenkiste, B. Van Waeyenberge, and V. V. Kruglyak, Phys. Rev. Lett. **110**, 097201 (2013)

[17] C. T. Boone, J. A. Katine, J. R. Childress, V. Tiberkevich, A. Slavin, J. Zhu, X. Cheng, I. N. Krivorotov, Phys. Rev. Lett. **103**, 167601 (2009)

[18] A. N. Slavin , I. N. Krivorotov, United States Patent, US 7678475 B2, March 16, 2010.

[19] D.V. Berkov, Phys. Rev B. **87**, 014406 (2013)

[20] G. Consolo, L. Lopez-Diaz, L. Torres, B. Azzerboni, Phys. Rev. B **75**, 214428 (2007)

[21] G. Consolo, B. Azzerboni, G. Gerhart, G.A. Melkov, V. Tiberkevich, A.N. Slavin, Phys. Rev. B **76**, 144410 (2007)

[22] G. Consolo, B. Azzerboni, G. Finocchio, L. Lopez-Diaz, L. Torres, J. Appl. Phys. **101**, 09C108 (2007)

[23] A.N. Slavin and V.S. Tiberkevich, IEEE Trans. Magn. **44**, 1916 (2008)

[24] A. Romeo, G. Finocchio, M. Carpentieri, L. Torres, G. Consolo, B. Azzerboni, Physica B **403**, 464 (2008)

[25] G. Consolo, L. Torres, L. Lopez-Diaz, B. Azzerboni, IEEE Trans. Magn. **43**, 2827 (2007).

[26] Du-Xing Chen, E. Pardo and A. Sanchez, IEEE Trans. Magn. **38**, 1742 (2002).